

Aerial transport of bacteria by dust plumes in the Eastern Mediterranean revealed by complementary rRNA/rRNA-gene sequencing

Burak Adnan Erkorkmaz ¹, Daniella Gat ¹ & Yinon Rudich ¹ 

Processes influencing the transport of airborne bacterial communities in the atmosphere are poorly understood. Here, we report comprehensive and quantitative evidence of the key factors influencing the transport of airborne bacterial communities by dust plumes in the Eastern Mediterranean. We extracted DNA and RNA from size-resolved aerosols sampled from air masses of different origins, followed by qPCR and high-throughput amplicon sequencing of 16S ribosomal RNA gene and transcripts. We find that airborne bacterial community composition varied with air mass origin and particle size. Bacterial abundance, alpha diversity and species richness were higher in terrestrially influenced air masses than in marine-influenced air masses and higher in the coarse particle fraction (3.0 to 10.0 μm) than in the fine fraction (0.49 to 1.5 μm). This suggests that airborne bacteria mainly were associated with dust particles or transported as cell aggregates. High abundances of rRNA from human, animal and plant pathogen taxa indicate potential ecological impacts of atmospheric bacterial transport.

¹Department of Earth and Planetary Sciences, Weizmann Institute of Science, Rehovot 7610001, Israel. email: yinon.rudich@weizmann.ac.il

Windblown dust can carry microorganisms over great distances^{1–6}. Airborne microbial communities transported by dust from various sources may significantly affect aquatic, atmospheric, and terrestrial ecosystems once the dust settles^{7–13}. Bacteria constitute the major fraction of microorganisms emitted to the atmosphere, and once airborne, they can serve as condensation and ice nuclei^{14–16} and participate in cloud water chemistry^{17–19}. In addition, transported pathogens may impact agriculture and human health^{13,20,21}. Airborne communities transported from various sources carry distinct and diverse taxa^{22–24}. Recent studies have suggested that the structure and composition of airborne microbial communities are strongly affected by seasonality^{25,26}, air mass origin, PM₁₀ concentration^{3,4,6}, meteorological conditions, aerosol chemical composition²⁷, and the size of the airborne particles^{6,28–30}.

Most recent studies of the airborne microbiome have applied high-throughput sequencing of the 16 S ribosomal RNA gene^{3–5} to characterize the phylogenetic and taxonomic diversity of the present community. At the same time, sequencing of the 16 S ribosomal RNA may provide additional information regarding the phylogeny and taxonomy of potentially active bacterial community³¹. Comparative analysis of the rRNA and the rRNA-encoding genes has recently provided meaningful ecological insights into terrestrial and aquatic environments regarding the interactions with the environment^{32–36}. However, less is known about the functional capacity of microbial communities transported in the atmosphere, primarily due to technical limitations such as low biomass, challenges in acquiring high-quality genetic material, and the lack of advanced molecular tools^{37–39}. A few studies have previously applied amplicon or metatranscriptome sequencing to ribosomal RNA or mRNA. They have revealed potentially active communities in the Arctic atmospheric ecosystem⁴⁰, in the atmosphere, and in cloud water sampled at a mountaintop research station where they likely influence the cycling of organic compounds^{18,41} and interfere with abiotic chemical processes⁴². From an ecological perspective, improving our knowledge about the aerial dispersal of potentially active bacterial communities is particularly important because it is a key process, along with selection, drift, and speciation, that control the patterns that drive the diversity, abundance, and composition of species in microbial communities⁴³ and thereby significantly affect the maintenance of the global biodiversity.

The Eastern Mediterranean (EM) Basin is a crossroad for various air masses of different origins. It experiences frequent dust storms in all seasons from the Sahara, the Arabian Peninsula, Iraq, and eastern Syrian deserts⁴⁴. Air masses transported from Europe are characterized by lower particulate matter concentrations with an aerodynamic diameter smaller than 10 μm (PM₁₀)⁴⁵. Thus, the EM Basin affords ample opportunities to identify and characterize the unique taxonomic signatures and information about the potential environmental impacts on the receptor region. Global climate change is projected to increase heat and drying processes in the Eastern Mediterranean and the Middle East regions resulting in elevated particulate matter concentrations and intensified dust event occurrences. These predictions further underscore the importance of studying the atmospheric transport of microbial communities on both global and regional scales^{46,47}.

Furthermore, understanding the variability in the airborne microbial composition across dust size fractions is highly relevant to public health and the environment. Smaller airborne particles (<2.5 μm in diameter) have more significant potential for long-range transport. They also pose a higher propensity for respiratory system infections because they are more likely to penetrate deeper into the lungs following inhalation^{48,49}.

Here, we present a comprehensive and comparative study investigating airborne bacterial communities transported from

different origins in the EM region using 16 S ribosomal RNA and RNA-gene high-throughput amplicon sequencing together with quantitative polymerase chain reaction (qPCR) measurements in a size-resolved manner. Using these tools, we investigated the community composition of airborne bacteria and compared these communities between the different air masses, particle-size classes and library types (i.e., rRNA gene and rRNA).

Results

Air mass back trajectories and the estimated origin of the dust.

During the sampling campaign, air mass back trajectories showed three main distinct transport patterns: from the northwest, southwest, and the east (Supplementary Table 1), and were classified accordingly. The dust origins were estimated based on back trajectory analysis, integrated with dust column mass density maps (Supplementary Movies 1–12) obtained from MODIS observations as was done in previous studies^{3–6,44}. The high concentrations of suspended particulate matter in the dust column maps that coincided with the air mass trajectories were assigned as the potential dust origin. Since we did not chemically characterize the particles in the aerosol samples, the effect of locally suspended particles during the dust storms was not discernable based on chemical speciation.

The sampling date, air mass, and PM₁₀ concentrations are presented in Table 1. The classification of the air masses is Northwest (NW), Southwest (SW) and East, which are associated with the three different primary dust sources in the Eastern Mediterranean: Iraq, eastern Syria, and the Arabian Peninsula (East), and the Sahara Desert (SW)⁴⁴. Two of these sources, the Sahara Desert and the Arabian Peninsula, are among the world's largest dust sources, accounting for more than 50% of global dust emissions^{50–52}. The NW air masses are associated with low PM₁₀ air masses with some contribution from the neighboring dust sources such as Sinai and Negev deserts and thus represent mostly local airborne microorganisms and/or long-range transport from Europe^{3,4,6}.

Community-level multivariate comparison. PCA ordinations of Euclidean distance between samples based on center log-ratio transformed ASV counts of bacterial communities are presented in Supplementary Fig. 1. The community structures based on rRNA and rRNA-gene showed high similarity. In both communities, samples representing the same back trajectories tended to cluster together, but the influence of sampling date and PM₁₀ concentration was evident.

Table 1 Sampling date, air mass and particulate matter concentration (PM₁₀).

Date	Air mass	Mean PM ₁₀ (μg m ⁻³)
25.10.2019	Southwest	24.4 ± 7.8
26.10.2019	Southwest	37.8 ± 12.3
28.10.2019	Northwest	35.5 ± 5.1
10.11.2019	East	74 ± 17.6*
13.11.2019	East	98.8 ± 18.2*
14.11.2019	Southwest	66.7 ± 10.6*
18.11.2019	East	60.7 ± 23.1*
26.11.2019	Southwest	119.9 ± 14.8*
11.12.2019	Southwest	33.9 ± 4.3
11.6.2020	Northwest	32.8 ± 6.5
24.06.2020	Northwest	35.1 ± 10.8
28.07.2020	Northwest	35.5 ± 13.3

PM₁₀ values represent the mean daily concentration of particulate matter measuring 10 μm or less in diameter on each sampling date. The mean values corresponding to a high PM₁₀ concentration (i.e., dusty days) represented by an asterisk (*) symbol.

According to the PERMANOVA test, the rRNA and rRNA-gene communities differed significantly, although only a small fraction of the total community variance was attributed to this parameter ($R^2 = 0.02$, $p < 0.001$). When examining the effect of the air mass, PM_{10} concentrations, size class and sampling date on rRNA and rRNA-gene communities separately, we found that all of these parameters significantly affected the community composition, with sampling date ($R^2 = 0.35$ and 0.22) and air mass ($R^2 = 0.20$ and 0.11 for rRNA and rRNA-gene communities) responsible for the greatest share of the total variance, followed by PM_{10} ($R^2 = 0.07$ and 0.06) and size class ($R^2 = 0.04$ and 0.08). The results are presented in Table 2.

Diversity and richness of the airborne bacterial communities.

The composition of the airborne bacterial communities is discussed in Supplementary Results. Alpha-diversity analyses, based on richness (observed number of ASVs) and Shannon–Wiener diversity index, were conducted on rRNA and rRNA-gene communities by air mass. The results are presented in Fig. 1.

Table 2 The results of PERMANOVA analysis on the terms: air mass, particle concentration, particle size, and sampling date, in this order.

	rRNA community		rRNA-gene community	
	R^2	p values	R^2	p values
Air mass	0.20	<0.001	0.11	<0.001
PM_{10} concentration	0.07	<0.001	0.06	<0.001
Particle-size class	0.04	<0.001	0.08	<0.001
Sampling date	0.35	<0.001	0.22	<0.001
Residual	0.34	-	0.53	-
Total	1.00	-	1.00	-

The PERMANOVA analysis identifies percentage of variance explained (i.e., R^2) by each variable and whether each factor have a significant effect. For instance, the R^2 value of 0.20 indicates that 20% of total variance is explained by the specified variable.

Similar patterns of richness and diversity between rRNA and rRNA gene of different air masses were observed. According to the Kruskal–Wallis test, different air masses differed significantly in the diversity and richness of both the rRNA and rRNA-gene communities (Kruskal–Wallis, richness $p < 0.001$ and $= 0.003$, diversity $p < 0.001$ and < 0.001 , respectively). Specifically, according to a Wilcoxon signed-rank test, diversity and richness were significantly higher in the SW and East than those with NW air masses in both rRNA and rRNA-gene communities. The diversity of the rRNA and rRNA-gene communities of the East air masses was significantly higher than that of the SW air masses (Supplementary Table 3).

We also compared the diversity and richness of the rRNA and rRNA-gene communities. According to the Kruskal–Wallis test results, the diversity of rRNA-gene communities differed significantly from that of rRNA communities ($p = 0.030$), but the observed richness did not ($p = 0.586$). Comparing the diversity of rRNA vs. that of rRNA-gene communities in each air mass source revealed no significant differences for the SW and East samples (Wilcoxon signed-rank test, $p > 0.05$); however, the diversity in rRNA community was significantly lower than that of rRNA-gene community in the NW air masses ($p = 0.041$), possibly due to small sample size.

When all the samples (i.e., rRNA and rRNA-gene communities) were divided according to the particle-size class (i.e., fine, intermediate, and coarse), the diversity and richness differed significantly (Kruskal–Wallis, $p = 0.046$ and 0.007). Specifically, the diversity and richness of the coarse particle-size class were significantly higher than those of the fine particle-size classes (Wilcoxon signed-rank test, $p = 0.049$ and 0.007). All p values are presented in Supplementary Table 4.

Quantitative PCR. Figure 2 describes the number of 16 S ribosomal RNA transcripts and gene copies per 1 m^{-3} of sampled air, based on qPCR results. Overall, we found that the rRNA transcripts were significantly more abundant than the rRNA gene copies. We also found significant differences in rRNA transcripts

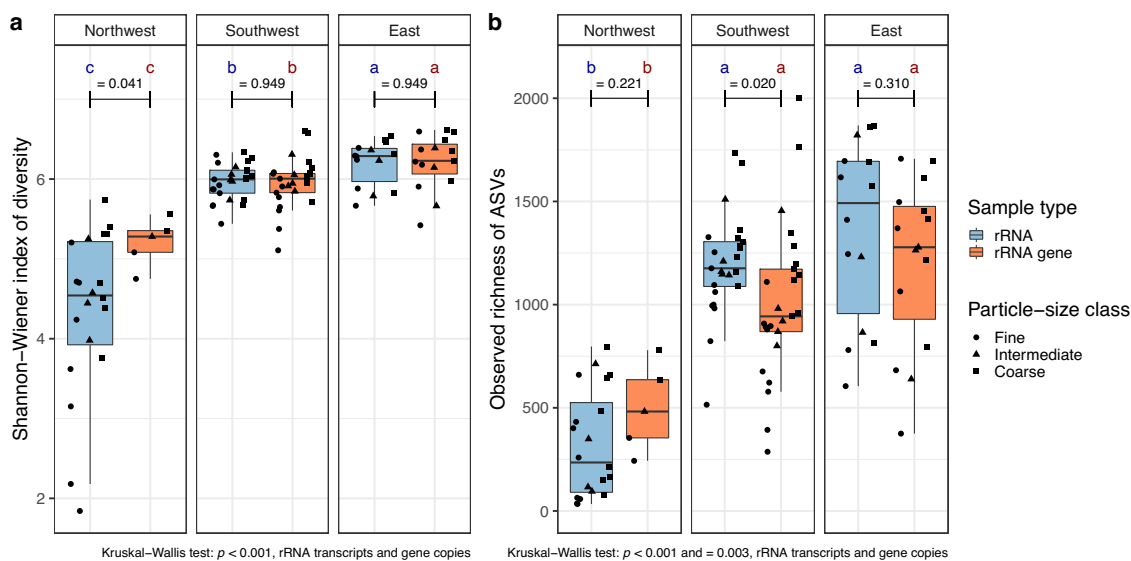


Fig. 1 Diversity and richness of airborne bacterial communities. Shannon–Wiener diversity indices (a), and observed richness (b) of rRNA and rRNA-gene communities of different air masses. Community type and particle-size classes are represented by different colors and symbol shapes, respectively. Box plot center lines represent the median values, the lower and upper hinges correspond to the first and third quartiles (the 25th and 75th percentiles), the lower and upper whisker extends from the hinge to the lowest and largest value no further than $1.5 \times \text{IQR}$ (interquartile range) from the hinge, and dots represent individual samples within each group. Lowercase letters indicate statistically significant differences ($p < 0.05$) between the air masses for rRNA and rRNA-gene communities separately. p values of significance between rRNA and rRNA-gene communities in each air mass are displayed over the horizontal bars in each plot.

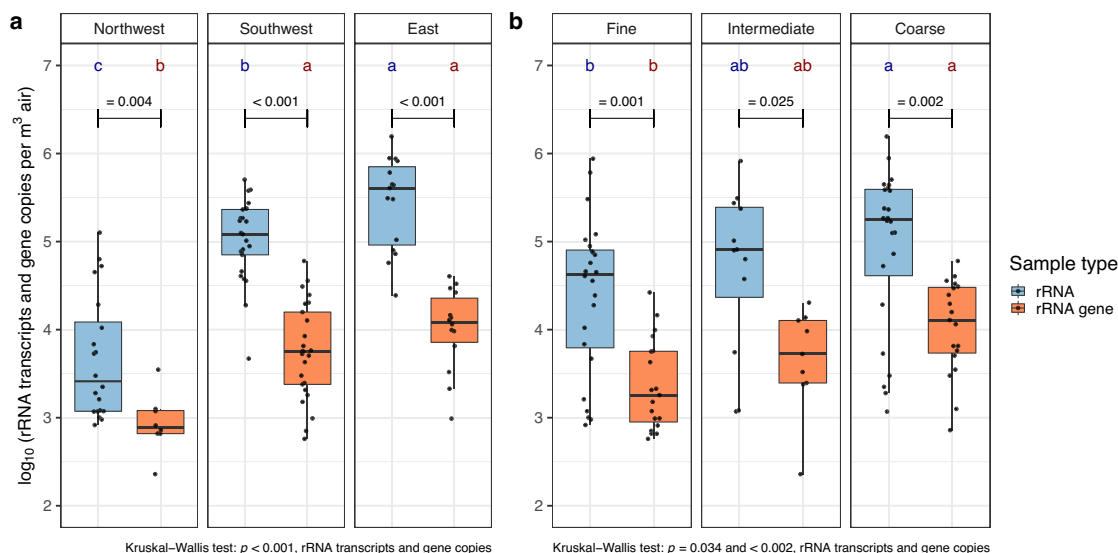


Fig. 2 Abundance of airborne bacterial communities. The rRNA transcripts and gene copies in different air masses (**a**), and particulate matter size classes (**b**). Box plot center lines represent the median values, the lower and upper hinges correspond to the first and third quartiles (the 25th and 75th percentiles), the lower and upper whisker extends from the hinge to the lowest and largest value no further than $1.5 \times \text{IQR}$ from the hinge, and dots represent individual samples within each group. Lowercase letters indicate significant differences ($p < 0.05$) between the air masses and particle-size classes for rRNA transcripts and gene copies, separately. p values of significance between rRNA transcripts and gene copies in each air mass and particle-size class are displayed over the horizontal bars in each plot.

and gene copies between air masses and particle-size classes (Supplementary Table 5). The East and SW air masses showed a higher abundance of rRNA transcripts and gene copies than the NW (Wilcoxon signed-rank tests, East $p < 0.001$ for rRNA transcripts and gene copies, respectively; and SW $p < 0.001$ and $p = 0.001$ for rRNA transcripts and gene copies, respectively). Significant differences in the abundances of rRNA transcripts were also observed among the airborne communities between the East and SW ($p = 0.015$), the former with higher rRNA abundance. Lastly, rRNA transcripts and rRNA gene copies were significantly more abundant in the coarse particle-size class compared to the fine particle-size class ($p = 0.021$ and 0.002 , respectively). The mean 16S rRNA transcripts and gene copies in each group are given in Supplementary Table 6.

Bacterial taxa associated with different air masses. We examined the taxa significantly associated with different air masses using a linear mixed model (MaAsLin2), as described in the “Methods” section, with the reference community defined as NW. The results are shown in Fig. 3. A total of 3458 unique ASVs were significantly associated with at least one of the air masses ($p < 0.05$, Benjamini–Hochberg correction for multiple comparisons). A total of 790 and 814 ASVs were associated with SW and East air masses compared to the NW, whereas 1311 and 1379 ASVs were associated with NW compared to the SW and East air masses, respectively. ASVs of Actinobacteriota, Bacteroidota, Firmicutes and Proteobacteria were most commonly associated with the air mass origin.

SW air masses were mainly characterized by elevated levels of Actinobacteria (202 ASVs of 816), Bacilli (165 ASVs of 515), Clostridia (207 ASVs of 784) and Negativicutes (9 ASVs of 22); East air masses by Actinobacteria (237 ASVs of 816), Chloroflexia (30 ASVs of 114), Gemmatimonadetes (8 ASVs of 43), Longimicrobia (8 ASVs of 36) and Rubrobacteria (11 ASVs of 29). Alphaproteobacteria (290 and 217 ASVs of 823), Bacteroidia (236 and 246 ASVs of 809) and Gammaproteobacteria (110 and 163 ASVs of 470) were the class of ASVs, among many others, associated with NW compared to SW and East air masses,

respectively. However, none of these dominating bacterial classes were uniquely associated only with one of the air masses (*i.e.*, the SW and East compared to the NW).

Bacterial taxa associated with different particle-size classes. We investigated the taxa associated with different particle-size classes, defining the fine particle-size class as the reference community. A total of 165 ASVs were significantly associated with at least one of the particle-size classes ($p < 0.05$, Benjamini–Hochberg correction for multiple comparisons). In total, 54 and 9 ASVs were associated with the coarse and intermediate particle-size classes, respectively, whereas 97 and 5 ASVs were associated with fine particle-size class (compared to coarse and intermediate, respectively). Significant ASVs associated with the coarse vs the fine particle-size classes are shown in Fig. 4. We found that the families Rhodobacteraceae and Oxalobacteraceae, among others, were only associated with coarse particles. In contrast, Sphingomonadaceae, WD2101 soil group, Hymenobacteraceae, Pseudonocardiaceae, Rubrobacteriaceae and Streptomycetaceae were only associated with fine particle-size class. Moreover, 13.4% (13 ASVs of 97) and 40.0% (2 ASVs of 5) of the total ASVs were associated with the fine particle-size class (*vs* the coarse and intermediate size class, respectively) were genera of *Streptomyces*.

Bacterial taxa associated with PM₁₀ concentration. We identified a total of 1831 unique ASVs that associated with PM₁₀ concentrations ($p < 0.05$, Benjamini–Hochberg correction for multiple comparisons). 42.3% (774 ASVs of 1831) of these ASVs were identified with a positive coefficient, indicating that the abundance of these taxa increased with the increase in PM₁₀ concentrations, whereas 57.7% (1057 ASVs of 1831) ASVs were identified with a negative coefficient, indicating that the abundance of these taxa decreased with the increase in PM₁₀ concentrations. These results are shown in Fig. 5. Actinobacteria (27.0%, 220 ASVs of 816), Alphaproteobacteria (23.0%, 189 ASVs of 823), Chloroflexia (14.0%, 16 ASVs of 114) and Thermoleophilia (12.5%, 16 ASVs of 128) ASVs tended to increase in abundance with the increasing in PM₁₀ concentrations whereas

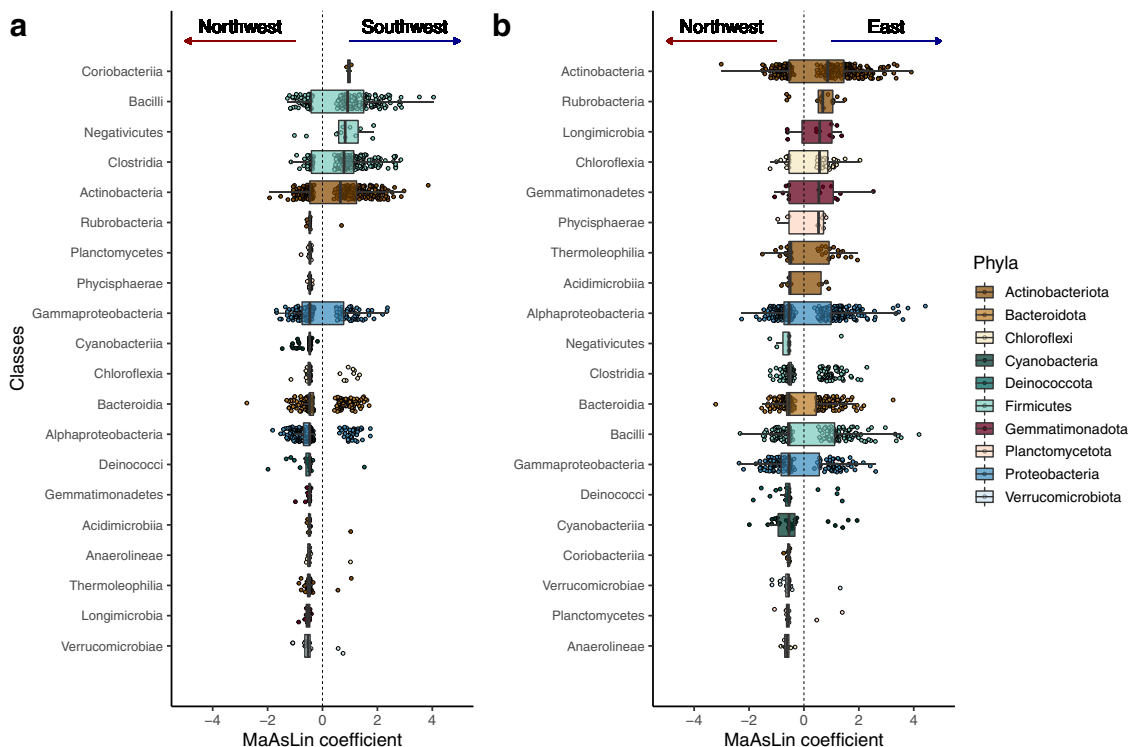


Fig. 3 Bacterial taxa significantly associated with different air masses. The MaAsLin2 scores per class is presented with association to the NW and the SW (a), and the NW and the East (b) trajectories. Each color represents a different phylum. Box plot center lines represent the median values, the lower and upper hinges correspond to the first and third quartiles (the 25th and 75th percentiles), the lower and upper whisker extends from the hinge to the lowest and largest value no further than 1.5 * IQR from the hinge, and dots represent ASVs within each group. Bacterial classes with more than ten ASVs associated with one of the air masses are shown.

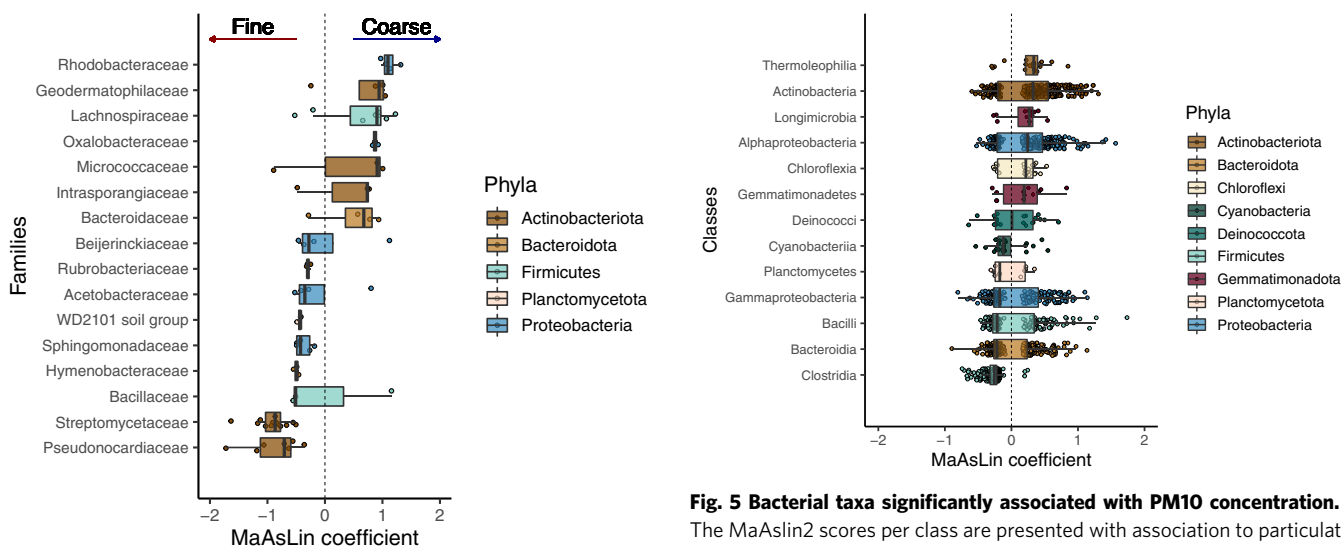


Fig. 4 Bacterial taxa significantly associated with coarse particle-size class compared with fine particle-size class. The MaAsLin2 scores per family is presented with association to fine and coarse particle sizes. Each color represents a different phylum. Box plot center lines represent the median values, the lower and upper hinges correspond to the first and third quartiles (the 25th and 75th percentiles), the lower and upper whisker extends from the hinge to the lowest and largest value no further than 1.5 * IQR from the hinge, and dots represent ASVs within each group. Bacterial families with more than two ASVs associated with one of the particle-size are shown.

Fig. 5 Bacterial taxa significantly associated with PM10 concentration. The MaAsLin2 scores per class are presented with association to particulate matter concentration. Each color represents a different phylum. Box plot center lines represent the median values, the lower and upper hinges correspond to the first and third quartiles (the 25th and 75th percentiles), the lower and upper whisker extends from the hinge to the lowest and largest value no further than 1.5 * IQR from the hinge, and dots represent ASVs within each group. Bacterial classes with more than ten ASVs associated with PM₁₀ concentration are shown.

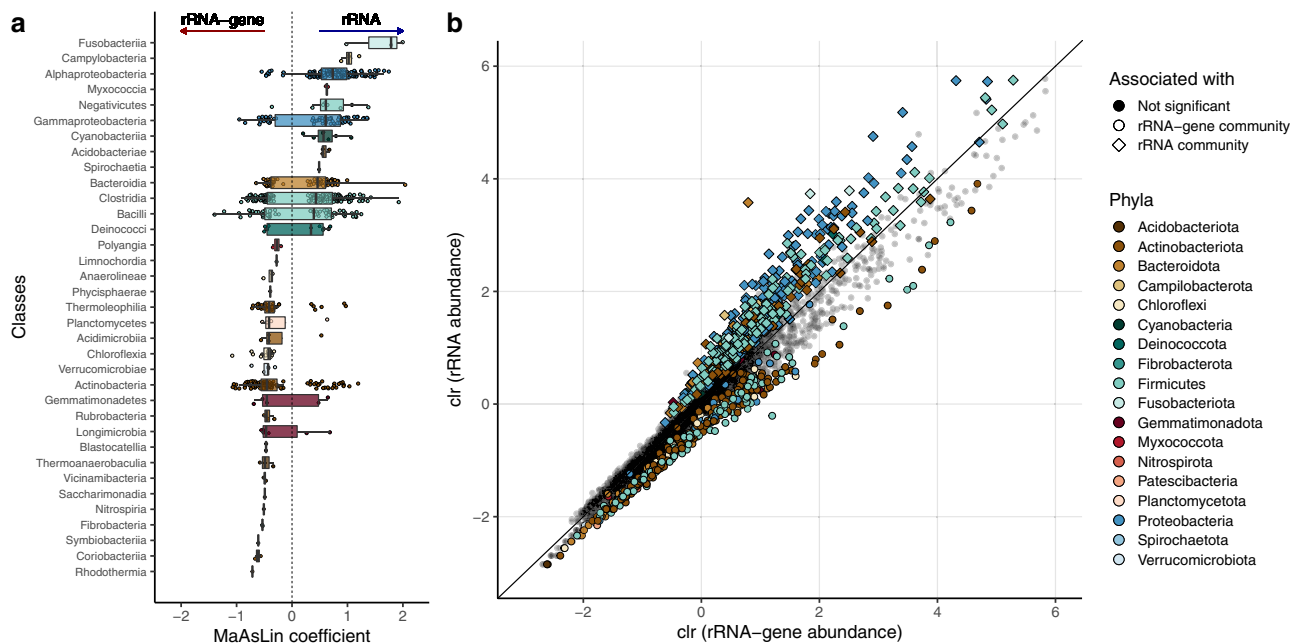


Fig. 6 Bacterial taxa significantly associated with rRNA vs. rRNA-gene communities. **a** The MaAsLin2 scores per class are presented with association to rRNA and rRNA-gene communities. Each color represents a different phylum. Box plot center lines represent the median values, the lower and upper hinges correspond to the first and third quartiles (the 25th and 75th percentiles), the lower and upper whisker extends from the hinge to the lowest and largest value no further than $1.5 \times \text{IQR}$ from the hinge, and dots represent ASVs within each group. **b** ASV mean abundance (represented by clr-transformed counts) of rRNA (vertical axis) and rRNA-gene (horizontal axis). Each dot represents a different ASV. Significant results for ASVs with high rRNA abundance are depicted by colored diamonds, whereas ASVs with low rRNA abundance are shown as colored dots; each color represents a different phylum. The diagonal line represents the 1:1 ratio between rRNA to rRNA-gene abundance.

Bacilli (%21.2%, 109 ASVs of 515), Bacteroidia (23.5%, 190 ASVs of 809), Clostridia (40.7%, 319 ASVs of 784) and Cyanobacteriia (26.9%, 18 ASVs of 67) ASVs tended to decrease in abundance with increasing PM_{10} concentrations.

Bacterial taxa associated with rRNA and rRNA-gene communities. We examined the taxa associated with rRNA and rRNA-gene communities, as a proxy for ASVs with significantly higher and lower rRNA abundance than their rRNA-gene abundance. Results are presented in Fig. 6. Overall, 478 ASVs were identified with a significantly higher rRNA abundance, whereas 363 ASVs had a significantly lower rRNA abundance ($p < 0.05$, Benjamini-Hochberg correction for multiple comparisons), compared with rRNA-gene abundance. Alphaproteobacteria and Gammaproteobacteria were the two dominating classes, in which 19.0% (156 out of a total of 832 ASVs) and 11% (52 out of a total of 470 ASVs) of their total ASVs, respectively, displayed high rRNA abundance. A few ASVs of these classes displayed low rRNA abundance (0.01%, and 0.04%, for Alpha- and Gammaproteobacteria, respectively). Other dominating class such as Actinobacteria, Chloroflexia and Thermoleophilia were more commonly associated with low rRNA abundance (11.0%, 90 ASVs of 816; 16.6%, 19 ASVs of 114; 25.8%, 33 ASVs of 128, respectively) than with high rRNA abundance (0.02%, 24 ASVs of 816; 0.00%, zero ASVs of 114; 0.04%, 6 ASVs of 128).

Furthermore, we investigated whether the abundant (i.e., clr rRNA-gene abundance > 0) or rare (i.e., clr rRNA-gene abundance < 0) taxa could have a high rRNA abundance and these results are presented in Supplementary Results.

Discussion

Factors influencing the airborne bacterial community structure. The bacterial communities, as detected by 16S rRNA and rRNA-gene sequencing, varied in composition across all collected samples according to their air mass source. According to

PERMANOVA analysis, the sampling date and air mass were the two key variables responsible for the observed variance across all samples and the main environmental driver structuring the airborne community composition and assembly in both the rRNA and rRNA-gene samples. Particulate matter concentration and size class were the other two significant variables affecting the variance in airborne communities. These findings are consistent with findings in previous studies^{3,4,6}.

A higher proportion of total variance was explained by the measured environmental variables (i.e., sampling date, air mass, particulate matter size class, and concentrations) in rRNA communities ($R^2 = 0.66$) than in the rRNA-gene communities ($R^2 = 0.47$). This may be expected since the copies per genome of a cell's ribosomal RNA gene generally can vary between 1 and 15^{53} , whereas the number of transcripts synthesized per cell may reach up to thousands depending on the cellular metabolic state and nutrient availability⁵⁴⁻⁵⁶.

The abundance (i.e., rRNA gene copies and rRNA transcripts), alpha diversity and richness of samples of the NW trajectories were significantly lower than those of all other samples, suggesting that the communities coming from the terrestrial sources are more abundant and diverse. This is consistent with the findings of previous studies at the same sampling location. These studies suggested that the NW air masses, are characterized by lower PM_{10} concentrations and likely represent the local bacterial communities^{3,4,6}. Moreover, the greater abundance, diversity and richness observed in aerosol samples of the coarse particles compared to the fine particles indicate that most of the airborne bacteria are attached to mineral dust or transported as cell aggregate.

To the best of our knowledge, this is the first comprehensive survey to characterize airborne bacteria in the atmosphere in a size-resolved manner using rRNA and rRNA-gene sequencing. The higher yield of rRNA, along with its potential implications on

the recent activity of the sampled bacteria, may prove to be a more reliable method than rRNA-gene for airborne community analysis. The greater sensitivity displayed by rRNA transcripts to environmental parameters such as air mass source, PM₁₀ concentration, etc., suggests that the rRNA library is less affected by relic nucleic acids than the rRNA-gene library, possibly due to faster degradation of rRNA compared with rRNA-gene, albeit slower than the degradation of mRNA.

Effect of air mass source on bacterial community composition.

Animal and human commensal genera such as aerobic (most species) *Corynebacterium*⁵⁷, strictly anaerobic, non-spore-forming *Bacteroides*⁵⁸, aerotolerant-anaerobic or microaerophilic, non-spore-forming *Lactobacillus*⁵⁹, obligately anaerobic *Oscillospiraceae* UCG-005⁶⁰, *Ruminococcus torques* group⁶¹ *Christensenellaceae* R-7 group⁶², and aerobic, spore-forming, halotolerant and soil, marine and hypersaline environments-dwelling *Nocardiopsis*⁶³, soil-dwelling, spore-forming *Streptomyces*⁶⁴ were abundantly associated with SW air masses.

Calcareous carbonaceous rocks (e.g., marble, limestone, and calcarenite)-dwelling, desiccation, solar radiation, salt and metal resistant bacterial genera of *Geodermatophilus*⁶⁵, soil, water and air-dwelling bacterial genera of *Adhaeribacter*⁶⁶, free-living, aerobic, nitrogen-fixing, soil and plant rhizosphere and phyllosphere-dwelling bacterial genera of *Microvirga*⁶⁷, soil-dwelling, spore-forming *Streptomyces*⁶⁴, soil-dwelling bacterial genera of *Nocardioides*⁶⁸, animal and human commensal, aerobic (most species) genera of *Corynebacterium*⁵⁷ were abundantly associated with East air masses.

Strictly aerobic, ice-nucleation active *Sphingomonas*^{8,69}, nitrate-reducing, extremophile soil bacterial genera of *Paracoccus*⁷⁰, aerobic and non-spore forming *Pseudomonas*⁷¹, soil, water and air-dwelling bacterial genera of *Roseomonas*⁷², mesophilic or thermophilic, aerobic, ionizing-radiation resistant bacterial genera of *Deinococcus*⁷³ were some of the dominating genera were associated with the NW air masses. These genera are abundantly found in aquatic habitats^{74–77} and in aerosol samples collected in clear atmospheric conditions^{40,42} in previous studies.

Although the number of aerosol samples in this study was limited to three to five samples per air mass, we identified unique taxonomic signatures for each air mass representative of the potential source. The airborne bacterial community of the NW air masses were more affected by marine ecosystem though, some contribution of terrestrial origins was evident, whereas the SW and East air masses were dominated by terrestrial origins, inferred by the 16S rRNA and rRNA gene sequencing. These results are consistent with the back trajectory analysis and dust column density maps. The NW air masses, showed mostly a marine trajectory over the Mediterranean Sea with some terrestrial contribution from the neighboring regions such a Sinai and Negev deserts; whereas the SW and East air masses were characterized by high PM₁₀ concentrations (except for three SW aerosol samples) that are typical of dust storms in the Eastern Mediterranean often originating from Saharan desert, with a possible contribution of the Sinai and Negev deserts (SW)^{78,79}, the Arabian Peninsula, Iraq, eastern Syria and Jordan (East)⁴⁴. Moreover, majority of ASVs both associated with air mass (i.e., SW and East) and PM₁₀ (SW: 83.1%, 158 ASVs of 190; East: 84.8%, 395 ASVs of 466), positively correlated with the increase in PM₁₀ concentrations, suggesting that the origin of SW and East air masses are more likely to be deserts. We also tracked the potential environmental source of airborne bacteria using dbBact⁸⁰. According to the results, ASVs that are negatively correlated with the increasing PM₁₀ concentrations displayed enriched ontology terms associated with fecal bacteria from

human and farm animals whereas ASVs that are positively correlated with the increasing PM₁₀ concentrations showed enriched ontology terms associated with desert and soil bacteria. This indicates that dust plumes bring desert and soil-associated bacteria over great distances to the EM.

Some of the signature taxa such as *Microvirga*, *Geodermatophilus* and *Corynebacterium* previously identified in East air masses sampled at the same sampling location, using a different aerosol sampling device (i.e., microorifice uniform deposit impactor, MOUDI) and sequencing technique (i.e., based on only rRNA gene)⁶. Other index taxa such as *Jeotgalicoccus* identified in East air masses in the same previous study however, was associated with both SW and East (to a lesser extent) air masses in this study. The observed taxonomic differences between the two studies at the same sampling location may be a result of natural variance or different sampling and sequencing techniques used.

The bacterial genera *Acinetobacter*, *Corynebacterium*, *Lactobacillus*, *Methylobacterium*, *Pseudomonas* and *Sphingomonas* genera were reported to be possible contaminants, especially in samples obtained from low-biomass environments⁸¹. We found a higher number of ASV affiliated with these taxa in collected dust samples (i.e., SW and East) than in the NW samples. This observation indicates that these bacteria were more likely to be transported by the dust.

Effect of particle-size class on bacterial community composition.

Understanding the relationship between the ecology and lifestyle of specific taxa and particle-size class can provide meaningful insights into the aerial dispersal patterns of bacteria. For example, many ASVs of soil-dwelling bacterial families were significantly associated with the fine particle-size class, including the family Streptomycetaceae⁶⁴ (31.3%, 15 ASVs of 48), specifically genera *Streptomyces* (39.3%, 13 ASVs of 33); and the family Pseudonocardiaceae⁸² (10.1%, 9 ASVs of 89) including the genera *Actinomycetospira*, *Actinophytocola*, *Amycolatopsis*, *Lechevalieria*, *Saccharothrix* and *Umezawaea*. These two families alone comprise approximately 25% (24 ASVs of 97) of all fine particle-associated bacteria (compared to the coarse particles). These bacterial families exhibit a life cycle that is similar to many fungi that involve the formation of hyphal filaments from the vegetative mycelium during colony growth, followed by sporulation, aerial segregation (as single cells i.e., spores) and germination in a new environment^{64,82}. Some of the families that were only associated with fine particle-size class such as Hymenobacteraceae (*Adhaeribacter*, *Hymenobacter* and *Pontibacter*), Rubrobacteriaceae (*Rubrobacter*), Sphingomonadaceae (Ellin6055, *Novosphingobium* and *Sphingomonas*) and WD2101 soil group are known biofilm-dwelling bacteria in various environments^{83–87}. This suggests that during the emission or aerial transport, cell aggregates are detached and dispersed as individual cells.

Animal and human commensal families such as Lachnospiraceae (*Ruminococcus torques* group, CHKCI001, GCA-900066575 and UCG-010)⁸⁸ and Bacteroidaceae (*Bacteroides*)⁵⁸, soil-dwelling families Geodermatophilaceae (*Klenkia* and *Geodermatophilus*)⁶⁵ and Oxalobacteraceae (*Noviherbaspirillum* and *Massilia*)⁸⁹, air and human skin residing Micrococaceae (*Kocuria*, *Nesterenkonia* and *Yaniella*)⁹⁰ and nitrate-reducing, extremophile soil bacterial family Rhodobacteraceae (*Paracoccus*)⁷⁰ were associated with coarse particle-size class. Many of these genera form cell aggregates or produce extracellular polymeric substances^{91–95}. Altogether, the results suggest that the ecology and specific lifestyle of bacteria in their source environment may have strong influence on observed aerial transport patterns (i.e., as single cells or cell aggregates).

Bacterial taxa with high rRNA abundance. Our results show that the rRNA:rRNA gene ratios (inferred by qPCR) were

between 2.5 and 276.3 ($M = 31.95$, $SD = 41.50$) in all samples, and when grouped according to air mass and particle-size class, rRNA transcripts were significantly more abundant than rRNA gene copies. The observed 16S rRNA:rRNA gene ratios in our study were relatively lower than the findings of a previous study in the Arctic atmospheric ecosystem, which reported an average of 585 ± 288 16S rRNA transcripts per cell (accounting for an average of 4.02 ribosomal operons per cell)⁴⁰. This variation could result from different sampling (high volume impinger was operated for 5 h where atmospheric samples were collected into an RNA fixative solution) and the nucleic acids extraction methods (chemical and physical lysis were used together) or ecosystems studied.

We observed a range of distributions at the class level for taxa with high and low rRNA abundance. For example, Alphaproteobacteria (19.0%, 156 ASVs of 823) and Gammaproteobacteria (11.0%, 52 ASVs of 470) mostly represent the high-rRNA abundance ASVs, whereas Actinobacteria (11.0%, 90 ASVs of 816), Chloroflexia (16.6%, 19 ASVs of 114) and Thermoleophilia (25.8%, 33 ASVs of 128) mostly represent low-rRNA abundance ASVs. Other dominating classes such as Bacteroidia, Bacilli, and Clostridia did not exhibit such discernable traits at the class level. Previous studies attributed the bacterial low- and high-rRNA abundance to a phylogenetically conserved trait related to cell size⁹⁶ and habitat preference^{97,98}. In this study, we did not find a substantial relationship between bacterial cell size⁹⁹ and the rRNA content of specific taxa.

We identified 9.4% of total ASVs with a high-rRNA abundance (478 ASVs of 5,051). The dominating genera were the hydrocarbon-degrading, aerobic *Acinetobacter*¹⁰⁰ (1.9%, 9 ASVs of 478); strictly anaerobic, human and animal commensal *Bacteroides*⁵⁸ (2.7%, 13 ASVs of 478); facultative anaerobic, non-spore-forming *Corynebacterium*¹⁰¹ (1.9%, 9 ASVs of 478); aerobic *Hymenobacter*^{102,103} (2.1%, 10 ASVs of 478); aerotolerant-anaerobic or microaerophilic, non-spore-forming, human and animal commensal *Lactobacillus*⁵⁹ (2.9%, 14 ASVs of 478); facultative methylotroph *Methylobacterium-Methylorubrum*¹⁰⁴ (1.9%, 9 ASVs of 478); heterotrophic and nitrate-reducing *Paracoccus*⁷⁰ (3.6%, 17 ASVs of 478); aerobic and non-spore-forming *Pseudomonas*⁷¹ (3.8%, 18 ASVs of 478); anaerobic, human commensal *Ruminococcus torques* group¹⁰⁵ (2.9%, 14 ASVs of 478); and strictly aerobic, ice-nucleation active *Sphingomonas*^{8,69} (6.3%, 30 ASVs of 478); all are genera known widely distributed in nature, and isolated from various terrestrial and aquatic ecosystems. Species belonging to the genus of *Acinetobacter* (e.g., *A. baumannii*, *A. nosocomialis* and *A. pittii*)¹⁰⁶, *Bacteroides* (e.g., *B. distasonis*, *B. fragilis*, *B. ovatus*, *B. thetaiotaomicron* and *B. Vulgatus*)⁵⁸, *Corynebacterium* (e.g., *C. diphtheria*, *C. kutscheri*, *C. pseudotuberculosis* and *C. ulcerans*)^{107,108}, *Methylobacterium-Methylorubrum* (e.g., *M. extorquens*, *M. mesophilicum* and *M. zatmanii*)¹⁰⁹, *Paracoccus* (e.g., *P. yeii*)¹¹⁰, *Pseudomonas* (e.g., *P. aeruginosa*)¹¹¹ and *Sphingomonas* (e.g., *S. paucimobilis* and *S. suberifaciens*)^{112–116} are reported to be human, animal or plant pathogens. Their presence in the dust samples further emphasizes the potential ecological impact of aerial bacterial transport, as these may be human, animal and plant pathogens.

Viable microorganisms represent the functional capacity to drive ecosystem processes. Microbial growth and activity are linked to the ribosomes since they are the sole protein biosynthesis machinery of the cell. Specifically, in bacteria, ribosome biosynthesis is tightly regulated by ribosomal RNA transcription level in accordance with the current physiological state of the cell and in response to changing environmental conditions^{117–119}. However, there is no absolute correlation between the abundance of rRNA transcripts and the activity and growth of a cell. In fact, this relationship is likely to vary between

different bacteria due to different survival strategies³¹. In environmental samples, rRNA-based analyses, specifically 16S rRNA:rRNA gene ratios have been considered to indicate the current activity and growth. A higher ratio was assumed to be associated with high metabolic activity^{41,42,96,120,121}. However, this approach was criticized due to conflicting patterns between rRNA abundance and cell activity and growth in different species³¹. Moreover, rRNA transcripts can sometimes be detected for extended periods following cell death^{122–128}, although extracellular rRNA molecules are less likely to maintain long-term stability in harsh atmospheric conditions. However, this variability also raises concerns about using rRNA as a reliable indicator for viability and activity. Therefore, although our results may indicate that some of the airborne bacteria have been recently viable in the source environment or during the atmospheric transport, further studies by complementary methods are warranted to verify the viability¹²⁹ (e.g., culture-based techniques, cell staining for microscopy or flow cytometry) because of the uncertainties associated with the varying degradation time of rRNA in environment^{122–127} and the lack of systematic studies that evaluate the presence of rRNA for viability assessment¹³⁰.

The accurate quantification and identification of the taxa present in atmospheric samples rely on the sampling method used¹³¹. A potential limitation of this study was using impaction, which was previously shown to decrease the viability of the sampled microorganisms^{132,133}, for a relatively long sampling period in desiccation conditions. It is thus likely that some microorganisms might have been poorly represented by this study. The integrity of rRNA transcripts after cell death depends on the environmental conditions^{122–127}. Although the significantly higher rRNA transcripts (vs to rRNA gene copies) found in this study is consistent with the finding of a previous study where the aerosol sample of the Arctic atmospheric ecosystem was directly collected into a preservative solution⁴⁰, bioaerosol samples collected on quartz microfiber filters for a sampling period of 6 h may be subject to some bias due to the potential degradation of rRNA transcripts during the sampling.

Conclusions

It is often questioned whether the atmosphere is an active ecosystem capable of maintaining Earth's biodiversity and supporting the transport of viable bacteria and human, animal, and plant pathogens. Previous studies have suggested a continuous exchange of microorganisms between remote ecosystems, thus maintaining biodiversity and a healthy global ecosystem^{22,134–136}. Our results show that the composition of the airborne bacterial communities from different locations varies with diverse ecological significance. The air masses coming from terrestrial sources have significantly higher abundance, diversity and richness of bacteria than marine-influenced air masses in the Eastern Mediterranean. We found that the ecology and the specific lifestyle of the bacteria in the source environment may affect the aerial transport patterns (i.e., single cells or cell aggregates). The significantly higher abundance of bacteria, along with higher bacterial diversity and richness, in the coarse particle-size class suggests that most of the airborne bacteria are attached to mineral dust or transported as cell aggregates.

The greater sensitivity displayed by rRNA transcripts to environmental parameters suggests that rRNA library is less affected by relic nucleic acids than the rRNA-gene library. This highlights the importance of using a complementary approach i.e., rRNA and rRNA-gene sequencing in the future studies to acquire robust and more reliable data to understand the dynamic factors affecting the airborne community composition and assembly.

Although community composition and qPCR data may indicate the aerial transport of viable bacteria, further evidence based on cell integrity and cellular metabolism assay may help confirm this assumption. Some of the dominating bacteria that we identified with high-rRNA abundance are reported to be harmful to human, animal, and plant health. Thus potential atmospheric transport of pathogens may pose public and environmental health risks both regionally and globally. Future studies will focus on the transport of pathogens to determine their potential effect.

Materials and methods

Sample collection. Atmospheric PM₁₀ was collected on quartz microfiber filters (Whatman Sigma-Aldrich, Saint Louis, MO, USA, 203 mm × 254 mm for the backup stage, and Tisch Environmental, Inc., Cleves, OH, USA, TE-230-QZ Sotted Quartz Fiber for a five-stage high volume cascade impactor); all the filters were pre-baked at 450 °C for 5 h before sampling to rid them of all organic matter. Sampling was performed using a high-volume air sampler (Tisch Environmental, Inc., TE-6070X) at a flow rate of 67.96 m³ hr⁻¹ for six hours. Operating blanks were obtained following the same procedure but were placed in the sampler for only 5 min of operation.

A five-stage high-volume cascade impactor (Tisch Environmental, Inc., TE-235) was used to procure size-segregated samples (<0.49 μm, 0.49–0.95 μm, 0.95–1.5 μm, 1.5–3.0 μm, 3.0–7.2 μm, 7.2–10.0 μm). An equal air volume was sampled on each stage since the high-volume cascade impactor operates at an equal flow rate (i.e., 67.96 m³ hr⁻¹) per stage¹³⁷. All the samples were collected on the roof of a four-story building at the Weizmann Institute of Science, Rehovot, Israel (31.9070 N, 34.8102 E; 80 m AMSL). Sampling was designed to capture particulate matter from various sources (e.g., Sahara, Arabia, Syria) under varying concentrations (i.e., low and high PM₁₀)¹³⁸. Saharan dust storms frequently affect the EM Basin during winter and spring through cold-core mid-latitude Mediterranean and Sharav cyclones¹³⁹. In contrast, the dust storms originate from the Eastern sources, such as Iraq, eastern Syria, Jordan, and Saudi Arabia, mainly during the fall, are triggered by the main synoptic circulation system known as The Red Sea Trough¹⁴⁰. Thus, a specific period, from October to December, was chosen for collecting aerosol samples representing dust storms of different origins, while four aerosol samples representing clear conditions (i.e., low PM₁₀ Northwest air masses) were amassed from both dusty (i.e., winter to spring) and non-dusty seasons.

To achieve this sampling design, we followed various atmospheric forecast platforms (<https://www.windy.com/>; <https://forecast.uoa.gr/en/forecast-maps/dust/europe>; and <https://dust.aemet.es/forecast/nmmb-bsc-dust-forecast-sconce>) to predict and prepare for upcoming dust storms. These predictions were verified by the online PM₁₀ data of the Israeli Ministry of Environmental Protection database, Rehovot Air Monitoring station (<https://www.svivaqnm.net/>). Aerosol samples representing 12 different sampling days and PM₁₀ concentrations in a size-resolved manner (i.e., six different cutoff sizes) were obtained. At the end of each sampling event, the filters were cut using a sterile surgical scalpel and forceps and immediately submerged in RNA fixative solution (280 g L⁻¹ ammonium sulfate dissolved in 25 mM sodium sulfate solution with 10 mM EDTA, pH 5.2). All prepared batches of the RNA fixation solution were poured into several sterile Petri dishes in a biological hood and UV sterilized twice for 15 min each to eliminate potential nucleic acid contaminants. The samples were kept at -20 °C (for 3–5 days) until downstream processing. Since the direct extraction of nucleic acids from multiple samples following the long hours of nighttime sampling during the dust storms is challenging, we kept aerosol samples in an RNA fixation solution until the nucleic acids were extracted. This method was previously applied to bioaerosol samples, resulting in a successful microbial community analysis¹⁴¹. The extraction yields of nucleic acids and the microbial community analyses of frozen and instantly extracted (directly after sampling) ultra-low biomass aerosol samples showed no significant differences between the two methods in a previous study¹⁴². However, storing the samples at -20 °C before the extraction may lead to the loss of nucleic acids due to cell lysis, potentially leading to some bias in the community analysis depending on the cell type.

Particulate matter concentration data, backward trajectory analyses, and dust column mass density maps. Particulate matter concentration data were obtained from the Rehovot Air Monitoring station, located approximately 1 km from the sampling site. This station is part of the Israeli Ministry of Environmental Protection network. PM₁₀ concentration data were obtained in 5-min time intervals and were used to calculate the mean concentration for each sampling period.

To identify the origin of the sampled air mass, back trajectories were calculated using the hybrid single-particle Lagrangian integrated trajectory model (HYSPLIT)^{143,144} via the web interface (READY, http://ready.arl.noaa.gov/HYSPLIT_traj.php). Each back trajectory was calculated for 72 h at 3 different altitudes (0, 50, and 100 meters above ground level). The results are presented in Supplementary Table 1.

To identify the potential dust sources, time-averaged maps of dust column mass density (hourly 0.5° × 0.625°) and reanalysis meteorological data were acquired from the Modern-Era Retrospective analysis for Research and Applications

(MERRA-2) for each sampling event. Each retrospective analysis consisted of time-averaged hourly frames (i.e., maps of the given region) of dust column density maps for 72 h before the sampled event (including the sampling period) that were animated into short video clips for each sampling date (Supplementary Movies 1–12). Analyses and visualizations used in this study were produced with the Giovanni online data system developed and maintained by the NASA GES DISC¹⁴⁵.

Nucleic acid extraction and cDNA synthesis. DNA and RNA were coextracted from the filters using a PowerWater DNA isolation kit (Qiagen, Dresden, Germany) following the manufacturer's protocol, with the following adjustments. One piece of each filter (1 × 12 cm) was removed from the RNA-preserving solution and placed into separate bead tubes. One milliliter of PW1 solution was added to each tube, and the tubes were then vortexed horizontally for 5 min, followed by centrifugation at 2700 × g for 2 min. The supernatant from each bead tube was split into two aliquots and placed in 2 ml collection tubes. Then, we followed the manufacturer's protocol up to the last step (elution), which we repeated twice, using 50 μl of PW6 solution each time; the spin filter was soaked at room temperature for 5 min before centrifugation at 13,000 × g for 1 min. 100 μl of DNA/RNA solution per tube was obtained. Next, the DNA/RNA solution was split into two 50 μl aliquots. One of these aliquots was kept without further processing and was used in amplification and sequencing steps as a DNA sample.

The other 50 μl aliquot was treated with 1 μl DNase (DNase I, RNase-free, Thermo Fischer Scientific, Roskilde, Denmark) and incubated at 37 °C for 30 minutes to digest all the DNA. This reaction was repeated twice consecutively to remove any residues of DNA. This aliquot was used as an RNA sample for downstream reverse transcription and sequencing.

cDNA was synthesized from the RNA extracts using a High-Capacity cDNA Reverse Transcription Kit (Applied Biosystems, Life Technologies, CA, USA) with random primers. To ensure that all the DNA was digested in the previous step, we ran a control reaction for each sample to which no reverse transcriptase enzyme was added. These controls were treated according to the same protocol as the real reaction samples. No amplicons were evident after the quantitative polymerase chain reaction (qPCR), indicating that all DNA was digested.

The ribosomal RNA transcripts and gene copies in the aerosol samples were determined by qPCR (StepOnePlus Real-Time PCR, Applied Biosystems, Life Technologies) using RNA (RNA transcripts that were converted to cDNA as described above) and DNA extracts, respectively. qPCR in this study used universal bacterial primers, 331 F (TCCTACGGGAGGCAGCAGT) and 518 R (ATTACCGCGGCTGCTGG)¹⁴⁶, targeting a fragment of the small subunit of the bacterial ribosome (SSU), also referred to as the 16 S gene. qPCR reactions were performed in triplicate on each cDNA and DNA sample, including reverse transcriptase negative control reactions and non-template controls. Each 20 μl reaction mixture was prepared as follows: 10 μl of SensiFAST SYBR mix (Bioline, London, UK), 1 μM of each primer, 4 μl of molecular grade H₂O, and 2 μl of template gDNA or cDNA. The following thermal cycling conditions were used for amplification: 3 min at 95 °C followed by 35 cycles of 5 s at 95 °C and 20 s at 60 °C. A logarithmic calibration curve of known pNORM1 plasmid concentrations (designed by Christophe Merlin (LCPME, Nancy, France), synthesized by Eurofins Scientific) was used to quantify the nucleic acids as previously described³. Total ribosomal RNA transcripts and gene copies were normalized to the total volume of sampled air. A total of 129 samples representing rRNA and rRNA-gene of three air mass origins in 6 particle-size classes were analyzed, as follows: 24 and 10 samples of northwest; 30 and 30 of southwest; 17 and 18 of the east (rRNA and rRNA-gene, respectively).

A significant limitation in bioaerosol studies is the ultra-low biomass content of air samples¹⁴². Previous studies at the same location showed that aerosol samples, especially those with low PM₁₀ mass, contain very low amounts of genomic DNA (i.e., 16 S rRNA-gene copies)^{3–5}. However, when the number of different nucleic acids (i.e., 16 S rRNA transcripts and gene copies) was compared in a low biomass environment (i.e., Arctic atmospheric ecosystem) by qPCR, the number of RNA (i.e., 16 S rRNA transcripts) was always higher than the DNA¹³⁴. These results are in line with our initial nucleic acid extraction experiments in this study. Therefore, we used a DNA isolation kit for DNA/RNA co-extraction to specifically maximize the quantity and quality of the extracted DNA to obtain an applicable spectrum of airborne community DNA in this study. Although using a DNA isolation kit for DNA/RNA co-extraction may introduce recovery bias, comparing community diversity and richness of rRNA and rRNA-gene shows a good correlation for observed richness (Spearman's $\rho = 0.92$, $p < 0.001$) and diversity (Spearman's $\rho = 0.87$, $p < 0.001$), suggesting that this bias is small. However, the co-extraction of DNA and RNA will be re-examined in future studies, and a method that better suits both nucleic acids should be implemented.

Amplification and sequencing. The rRNA and rRNA-gene communities in the aerosol samples were analyzed by high-throughput amplicon sequencing (250 × 2 cycles) of 16 S ribosomal RNA and RNA-gene; RNA (RNA transcripts that were converted to cDNA) and DNA extracts were used as templates, respectively. The genomic sequencing was conducted at the DNA Sequencing Facility (DNAS) at the University of Illinois at Chicago (UIC) using an Illumina MiSeq instrument. The target sequence was a segment of the V4 region in the 16 S rRNA gene, amplified

using tagged bacterial/archaeal primers as follows: CS1_515F (ACACTGACGACATGTTCTACAGTGCCAGCMGCCGCGGTAA) and CS2_806R (TACGGTAGCAGAGACTTGGTCTGGACTACHVGGGTWCTAAT)¹⁴⁷. Short read length sequencing of the rRNA gene (i.e., V4 region in the 16S rRNA gene) may reduce the number of ASVs taxonomically classified¹⁴⁸. This may introduce some bias in the results.

Biostatistical microbiome data analysis. The sequencing data were analyzed using the R packages *DADA2* (version 1.16.0)¹⁴⁹ and *Phyloseq* (version 1.36.0)¹⁵⁰. Sequences (i.e., a total of 4,129,758) were quality-trimmed and filtered. Paired reads were merged, and chimeras were removed to produce amplicon sequence variants (ASVs). A total of 2,998,398 reads of bacterial 16S rRNA sequences (i.e., rRNA and rRNA-gene), including aerosol samples and blank filter controls (i.e., one for each particle-size class), were then assigned to 13,444 ASVs. Due to the low RNA and DNA quantities, not all samples were fit for biostatistical analysis. A total of 125 samples representing rRNA and rRNA-gene of three air mass origins in 6 particle-size classes were analyzed, as follows: 24 and 6 samples of northwest; 30 and 30 of southwest; 17 and 18 of the east (rRNA and rRNA-gene, respectively).

Taxonomic classification of the obtained ASVs was performed using the SSURef SILVA database (v.138)¹⁵¹. The contaminating sequences were identified using the *decontam* package relying on sequence frequencies¹⁵². Identified contaminant sequences were subsequently removed from the dataset. We also removed sequences that corresponded with *Chloroplasts* and *Mitochondria* as well as ambiguous and unclassified phylum annotations. The rRNA and rRNA-gene samples from each sampling date were treated as separate communities for all subsequent processing. ASVs with a read count lower than 5 in each sample and with a prevalence (i.e., number of samples each ASV occurs in) lower than 3 in the entire dataset were removed to avoid a small mean and trivially large coefficient of variation. Phantom taxa, defined as ASVs only observed in rRNA and not in rRNA-gene communities⁴², were also removed from the entire sampling event (Supplementary Methods). A total of 5,051 ASVs passed all filtration steps and were used in the subsequent biostatistical and community composition analyses. To account for data compositionality^{153,154}, zero counts were replaced using the *cmultRepl* function in the *zCompositions* (version 1.3.4) package based on geometric Bayesian multiplicative replacement followed by centered log-ratio (clr) transformation with the *clr* function in the *compositions* package¹⁵⁵. All statistical and model-based analyses were run using *clr*-transformed ASV counts unless otherwise noted.

The different particle size fractions were combined into four size classes: <0.49 μm —the backup stage; 0.49–1.5 μm (stage 4–5)—fine fraction; 1.5 to 3.0 μm (stages 3)—intermediate fraction and 3.0–10.0 μm (stages 1–2)—coarse fraction. These subgroups correspond to bacterial cell debris (backup stage), single cells (fine fraction), and cell aggregates (coarse fraction). The intermediate size class is more likely to represent cell aggregates than single cells, as the cell diameter of a single bacterial cell is typically between 0.7 to 1.5 μm (approximately 1 μm)¹⁵⁶. Due to the accumulation of cell debris and the bouncing effect on impactor stages¹⁵⁷, we excluded the backup stage (<0.49 μm) from further analysis (in qPCR and sequencing).

Variance analysis (PERMANOVA) was conducted using the *adonis2* function (1000 permutations) in the *vegan* package¹⁵⁸ based on the Euclidean dissimilarity matrix. PERMANOVA models were run separately using the following designs: (1) we examined the variance between rRNA and rRNA-gene communities over the entire dataset, and (2) we examined the variance explained by the variables air mass, particle concentration (PM₁₀), particle size, and sampling date, in this order, on rRNA and rRNA-gene communities. For both cases, blocks were defined as sample dates to account for the non-independence of different particle sizes sampled at the same time^{159,160}.

Richness (observed number of ASVs) and Shannon–Wiener diversity indices were calculated with the *Phyloseq* package¹⁵⁰. The Kruskal–Wallis rank-sum test and Wilcoxon signed-rank test were implemented for community richness, diversity, and qPCR analyses using the *stats* R package. In the Wilcoxon signed-rank test, *p* values were adjusted for multiple testing using the Benjamini–Hochberg method¹⁶¹.

ASVs that were significantly more abundant in the rRNA community than in the rRNA-gene community (1), in the SW and East air masses than the NW air mass (2), in the coarse and intermediate particle-size classes than the fine particle-size class (3) and with the increase in PM₁₀ concentrations (4) were identified using a linear mixed model of the *MaAsLin2* package¹⁶². The model was run separately for sample type (i.e., rRNA to rRNA-gene communities) (1), air-mass (2), particle-size class (3) and PM₁₀ concentration (4), with the following designs to examine significant associations between specific ASVs and each variable: (1) *fixed effect* = *c* (*sample type*), *random effect* = (*sample date*, *particle size*), (2;3;4) *fixed effect* = *c* (*air-mass*; *particle-size*; PM₁₀ concentration), *random effect* = (*sample type*, *sample date*). The reference communities were defined as the rRNA-gene (1), the NW air mass (2), and fine size class (3) in the models. All reported *p* values were corrected using the Benjamini–Hochberg method¹⁶¹, with adjusted *p* < 0.05 results considered significant. All modeling results are presented in Supplementary Table 2. Ontology-based enrichment analysis was conducted using *dbBact* database's differential abundance query mode to track the potential environmental source of the airborne bacteria⁸⁰.

Reporting summary. Further information on research design is available in the Nature Portfolio Reporting Summary linked to this article.

Data availability

Sequencing data are provided at the NCBI (SRA) database under the study accession code [PRJNA765143](https://doi.org/10.1038/s43247-023-00679-8). Supplementary Table 2 and 9 were deposited as data to suitable repository (<https://doi.org/10.5281/zenodo.7409699>).

Received: 27 February 2022; Accepted: 9 January 2023;

Published online: 06 February 2023

References

- Katra, I. et al. Richness and diversity in dust stormborne biomes at the Southeast Mediterranean. *Sci. Rep.* **4**, 5265 (2014).
- Kellogg, C. A. & Griffin, D. W. Aerobiology and the global transport of desert dust. *Trends Ecol. Evol.* **21**, 638–644 (2006).
- Mazar, Y., Cytryn, E., Erel, Y. & Rudich, Y. Effect of dust storms on the atmospheric microbiome in the eastern Mediterranean. *Environ. Sci. Technol.* **50**, 4194–4202 (2016).
- Gat, D., Mazar, Y., Cytryn, E. & Rudich, Y. Origin-dependent variations in the atmospheric microbiome community in Eastern Mediterranean Dust Storms. *Environ. Sci. Technol.* **51**, 6709–6718 (2017).
- Lang-Yona, N. et al. Links between airborne microbiome, meteorology, and chemical composition in northwestern Turkey. *Sci. Total Environ.* **725**, 138227 (2020).
- Gat, D. et al. Size-resolved community structure of bacteria and fungi transported by dust in the Middle East. *Front. Microbiol.* **12** (2021) <https://doi.org/10.3389/fmicb.2021.744117>.
- Hill, T. C. J. et al. Sources of organic ice nucleating particles in soils. *Atmos. Chem. Phys.* **16**, 7195–7211 (2016).
- Pandey, R. et al. Ice-nucleating bacteria control the order and dynamics of interfacial water. *Sci. Adv.* **2**, e1501630 (2016).
- Fröhlich-Nowoisky, J. et al. Ice nucleation activity in the widespread soil fungus *Mortierella alpina*. *Biogeosciences* **12**, 1057–1071 (2015).
- Estillore, A. D., Trueblood, J. V. & Grassian, V. H. Atmospheric chemistry of bioaerosols: heterogeneous and multiphase reactions with atmospheric oxidants and other trace gases. *Chem. Sci.* **7**, 6604–6616 (2016).
- Brodie, E. L. et al. Urban aerosols harbor diverse and dynamic bacterial populations. *Proc. Natl. Acad. Sci.* **104**, 299–304 (2007).
- Šantl-Temkiv, T. et al. Characterization of airborne ice-nucleation-active bacteria and bacterial fragments. *Atmos. Environ.* **109**, 105–117 (2015).
- Rahav, E., Ovadia, G., Paytan, A. & Herut, B. Contribution of airborne microbes to bacterial production and N₂ fixation in seawater upon aerosol deposition. *Geophys. Res. Lett.* **43**, 719–727 (2016).
- Failor, K. C., Schmale, D. G., Vinatzer, B. A. & Monteil, C. L. Ice nucleation active bacteria in precipitation are genetically diverse and nucleate ice by employing different mechanisms. *ISME J.* **11**, 2740–2753 (2017).
- de Araujo, G. G., Rodrigues, F., Gonçalves, F. L. T. & Galante, D. Survival and ice nucleation activity of *Pseudomonas syringae* strains exposed to simulated high-altitude atmospheric conditions. *Sci. Rep.* **9**, 7768 (2019).
- Lazaridis, M. Bacteria as Cloud Condensation Nuclei (CCN) in the Atmosphere. *Atmosphere* **10**, 786 (2019).
- Amato, P. et al. Active microorganisms thrive among extremely diverse communities in cloud water. *PLoS ONE* **12**, e0182869 (2017).
- Amato, P. et al. Metatranscriptomic exploration of microbial functioning in clouds. *Sci. Rep.* **9**, 4383 (2019).
- Vaitilingom, M. et al. Potential impact of microbial activity on the oxidant capacity and organic carbon budget in clouds. *Proc. Natl. Acad. Sci.* **110**, 559–564 (2013).
- Triadó-Margarit, X., Cáliz, J. & Casamayor, E. O. A long-term atmospheric baseline for intercontinental exchange of airborne pathogens. *Environ. Int.* **158**, 106916 (2022).
- Brodie, E. L. et al. Urban aerosols harbor diverse and dynamic bacterial populations. *Proc. Natl. Acad. Sci.* **104**, 299 (2007).
- Archer, S. D. J. et al. Airborne microbial transport limitation to isolated Antarctic soil habitats. *Nat. Microbiol.* **4**, 925–932 (2019).
- Mayol, E. et al. Long-range transport of airborne microbes over the global tropical and subtropical ocean. *Nat. Commun.* **8**, 201 (2017).
- Favet, J. et al. Microbial hitchhikers on intercontinental dust: catching a lift in Chad. *ISME J.* **7**, 850–867 (2013).
- Cáliz, J., Triadó-Margarit, X., Camarero, L. & Casamayor, E. O. A long-term survey unveils strong seasonal patterns in the airborne microbiome coupled to

- general and regional atmospheric circulations. *Proc. Natl. Acad. Sci.* **115**, 12229–12234 (2018).
26. Du, P., Du, R., Ren, W., Lu, Z. & Fu, P. Seasonal variation characteristic of inhalable microbial communities in PM2.5 in Beijing city, China. *Sci. Total Environ.* **610–611**, 308–315 (2018).
 27. Lang-Yona, N. et al. Links between airborne microbiome, meteorology, and chemical composition in northwestern Turkey. *Sci. Total Environ.* **725**, 138227 (2020).
 28. Gong, J., Qi, J., E, B., Yin, Y. & Gao, D. Concentration, viability and size distribution of bacteria in atmospheric bioaerosols under different types of pollution. *Environ. Pollut.* **257**, 113485 (2020).
 29. Zhang, T., Li, X., Wang, M., Chen, H. & Yao, M. Time- and size-resolved bacterial aerosol dynamics in highly polluted air: new clues for haze formation mechanism. *bioRxiv*, 513093 (2019) <https://doi.org/10.1101/513093>.
 30. Wei, M. et al. Size distribution of bioaerosols from biomass burning emissions: Characteristics of bacterial and fungal communities in submicron (PM1.0) and fine (PM2.5) particles. *Ecotoxicol. Environ. Saf.* **171**, 37–46 (2019).
 31. Blazewicz, S. J., Barnard, R. L., Daly, R. A. & Firestone, M. K. Evaluating rRNA as an indicator of microbial activity in environmental communities: limitations and uses. *Isme J.* **7**, 2061–2068 (2013).
 32. Barnard, R. L., Osborne, C. A. & Firestone, M. K. Responses of soil bacterial and fungal communities to extreme desiccation and rewetting. *ISME J.* **7**, 2229–2241 (2013).
 33. Schostag, M. et al. Distinct summer and winter bacterial communities in the active layer of Svalbard permafrost revealed by DNA- and RNA-based analyses. *Front. Microbiol.* **6** (2015) <https://doi.org/10.3389/fmicb.2015.00399>.
 34. Campbell, B. J., Yu, L., Heidelberg, J. F. & Kirchman, D. L. Activity of abundant and rare bacteria in a coastal ocean. *Proc. Natl. Acad. Sci.* **108**, 12776–12781 (2011).
 35. Deneff, V. J., Fujimoto, M., Berry, M. A. & Schmidt, M. L. Seasonal succession leads to habitat-dependent differentiation in ribosomal RNA:DNA Ratios among freshwater lake bacteria. *Front. Microbiol.* **7** (2016) <https://doi.org/10.3389/fmicb.2016.00606>.
 36. Zhang, Y., Zhao, Z., Dai, M., Jiao, N. & Herndl, G. J. Drivers shaping the diversity and biogeography of total and active bacterial communities in the South China Sea. *Mol. Ecol.* **23**, 2260–2274 (2014).
 37. Hospodsky, D., Yamamoto, N. & Peccia, J. Accuracy, precision, and method detection limits of quantitative PCR for airborne bacteria and fungi. *Appl Environ. Microbiol.* **76**, 7004–7012 (2010).
 38. Nieto-Caballero, M., Savage, N., Keady, P. & Hernandez, M. High fidelity recovery of airborne microbial genetic materials by direct condensation capture into genomic preservatives. *J. Microbiological Methods* **157**, 1–3 (2019).
 39. Behzad, H., Gojoberi, T. & Mineta, K. Challenges and opportunities of airborne metagenomics. *Genome Biol. Evol.* **7**, 1216–1226 (2015).
 40. Šantl-Temkiv, T., Gosewinkle, U., Starnawski, P., Lever, M. & Finster, K. Aeolian dispersal of bacteria in southwest Greenland: their sources, abundance, diversity and physiological states. *FEMS Microbiol. Ecol.* **94** (2018) <https://doi.org/10.1093/femsec/fiy031>.
 41. Klein, A. M., Bohannan, B. J. M., Jaffe, D. A., Levin, D. A. & Green, J. L. Molecular evidence for metabolically active bacteria in the atmosphere. *Front. Microbiol.* **7**, 772–772 (2016).
 42. Amato, P. et al. Active microorganisms thrive among extremely diverse communities in cloud water. *PLoS One* **12**, e0182869 (2017).
 43. Vellend, B. M. Conceptual synthesis in community ecology. *Q. Rev. Biol.* **85**, 183–206 (2010).
 44. Bodenheimer, S., Lensky, I. M. & Dayan, U. Characterization of Eastern Mediterranean dust storms by area of origin; North Africa vs. Arabian Peninsula. *Atmos. Environ.* **198**, 158–165 (2019).
 45. Kishcha, P., Volpov, E., Starobinets, B., Alpert, P. & Nickovic, S. Dust dry deposition over Israel. *Atmosphere* **11**, 197 (2020).
 46. Krasnov, H., Katra, I. & Friger, M. Increase in dust storm related PM10 concentrations: A time series analysis of 2001–2015. *Environ. Pollut.* **213**, 36–42 (2016).
 47. Zittis, G. et al. Climate change and weather extremes in the eastern Mediterranean and Middle East. *Rev. Geophysics* **60**, e2021RG000762 (2022).
 48. Griffin, D. W. Atmospheric movement of microorganisms in clouds of desert dust and implications for human health. *Clin. Microbiol. Rev.* **20**, 459–477 (2007).
 49. Prospero, J. M. Long-range transport of mineral dust in the global atmosphere: Impact of African dust on the environment of the southeastern United States. *Proc. Natl. Acad. Sci.* **96**, 3396–3403 (1999).
 50. Klingmüller, K., Pozzer, A., Metzger, S., Stenichikov, G. L. & Lelieveld, J. Aerosol optical depth trend over the Middle East. *Atmos. Chem. Phys.* **16**, 5063–5073 (2016).
 51. Notaro, M., Alkolibi, F., Fadda, E. & Bakhrjy, F. Trajectory analysis of Saudi Arabian dust storms. *J. Geophys. Res. Atmospheres* **118**, 6028–6043 (2013).
 52. Tegen, I. & Schepanski, K. The global distribution of mineral dust. *IOP Conf. Ser. Earth Environ. Sci.* **7**, 012001 (2009).
 53. Klappenbach, J. A., Saxman, P. R., Cole, J. R. & Schmidt, T. M. rrndb: the Ribosomal RNA Operon Copy Number Database. *Nucleic Acids Res.* **29**, 181–184 (2001).
 54. Bremer, H. & Dennis, P. P. Modulation of chemical composition and other parameters of the cell at different exponential growth rates. *EcoSal Plus* **3** (2008) <https://doi.org/10.1128/ecosal.5.2.3>.
 55. Schneider, D. A., Ross, W. & Gourse, R. L. Control of rRNA expression in *Escherichia coli*. *Curr. Opin. Microbiol.* **6**, 151–156 (2003).
 56. Gralla, J. D. *Escherichia coli* ribosomal RNA transcription: regulatory roles for ppGpp, NTPs, architectural proteins and a polymerase-binding protein. *Mol. Microbiol.* **55**, 973–977 (2005).
 57. Oliveira, A. et al. Insight of genus *Corynebacterium*: ascertaining the role of pathogenic and non-pathogenic species. *Front. Microbiol.* **8**, 1937–1937 (2017).
 58. Wexler, H. M. Bacteroides: the good, the bad, and the nitty-gritty. *Clin. Microbiol. Rev.* **20**, 593–621 (2007).
 59. Duar, R. M. et al. Lifestyles in transition: evolution and natural history of the genus *Lactobacillus*. *FEMS Microbiol. Rev.* **41**, S27–S48 (2017).
 60. Magzal, F. et al. Increased physical activity improves gut microbiota composition and reduces short-chain fatty acid concentrations in older adults with insomnia. *Sci. Rep.* **12**, 2265 (2022).
 61. Wang, L. et al. Increased abundance of *Sutterella* spp. and *Ruminococcus* torques in feces of children with autism spectrum disorder. *Mol. Autism* **4**, 42 (2013).
 62. Tavella, T. et al. Elevated gut microbiome abundance of Christensenellaceae, Porphyromonadaceae and Rikenellaceae is associated with reduced visceral adipose tissue and healthier metabolic profile in Italian elderly. *Gut microbes* **13**, 1–19 (2021).
 63. Bennur, T., Kumar, A. R., Zinjarde, S. & Javdekar, V. *Nocardiosis* species: Incidence, ecological roles and adaptations. *Microbiological Res.* **174**, 33–47 (2015).
 64. Jones, S. E. & Elliot, M. A. *Streptomyces* exploration: competition, volatile communication and new bacterial behaviours. *Trends Microbiol.* **25**, 522–531 (2017).
 65. Gtari, M. et al. Contrasted resistance of stone-dwelling Geodermatophilaceae species to stresses known to give rise to reactive oxygen species. *FEMS Microbiol. Ecol.* **80**, 566–577 (2012).
 66. Weon, H.-Y. et al. *Adhaeribacter aerophilus* sp. nov., *Adhaeribacter aerolatus* sp. nov. and *Segetibacter aerophilus* sp. nov., isolated from air samples. *Int. J. Syst. Evol. Microbiol.* **60**, 2424–2429 (2010).
 67. Marin, I. et al. 115-133 (Springer Berlin Heidelberg, 2014).
 68. Yoon, J.-H. et al. 1099-1113 (Springer New York, 2006).
 69. Steinberg, J. P. & Burd, E. M. In *Mandell, Douglas, and Bennett's Principles and Practice of Infectious Diseases* (Eighth Edition) (eds John E. Bennett, R. Dolin, & M. J. Blaser) 2667-2683.e2664 (W.B. Saunders, 2015).
 70. Kelly, D. P., et al. 232-249 (Springer New York, 2006).
 71. Silby, M. W., Winstanley, C., Godfrey, S. A. C., Levy, S. B. & Jackson, R. W. *Pseudomonas* genomes: diverse and adaptable. *FEMS Microbiol. Rev.* **35**, 652–680 (2011).
 72. Hyeon, J. W. & Jeon, C. O. *Roseomonas aerofrigidensis* sp. nov., isolated from an air conditioner. *Int. J. Syst. Evol. Microbiol.* **67**, 4039–4044 (2017).
 73. Battista, J. R. & Rainey, F. A. in *Bergey's Manual of Systematics of Archaea and Bacteria* 1-13.
 74. Angly, F. E. et al. Marine microbial communities of the Great Barrier Reef lagoon are influenced by riverine floodwaters and seasonal weather events. *PeerJ* **4**, e1511 (2016).
 75. Cárdenas, A., Rodríguez-R, L. M., Pizarro, V., Cadavid, L. F. & Arévalo-Ferro, C. Shifts in bacterial communities of two caribbean reef-building coral species affected by white plague disease. *ISME J.* **6**, 502–512 (2012).
 76. Kämpfer, P., Lodders, N., Huber, B., Falsen, E. & Busse, H. J. *Deinococcus aquatilis* sp. nov., isolated from water. *Int. J. Syst. Evol. Microbiol.* **58**, 2803–2806 (2008).
 77. Gallego, V., Sánchez-Porro, C., García, M. T. & Ventosa, A. *Roseomonas aquatica* sp. nov., isolated from drinking water. *Int. J. Syst. Evol. Microbiol.* **56**, 2291–2295 (2006).
 78. Roskin, J., Katra, I. & Blumberg, D. G. Particle-size fractionation of eolian sand along the Sinai-Negev erg of Egypt and Israel. *GSA Bull.* **126**, 47–65 (2014).
 79. Ganor, E. & Foner, H. A. Mineral dust concentrations, deposition fluxes and deposition velocities in dust episodes over Israel. *J. Geophys. Res.: Atmospheres* **106**, 18431–18437 (2001).
 80. Amir, A., Ozel, E., Haberman, Y. & Shental, N. Achieving pan-microbiome biological insights via the dbBact knowledge base. *bioRxiv*, 2022.2002.2027.482174 (2022) <https://doi.org/10.1101/2022.02.27.482174>.
 81. Eisenhofer, R. et al. Contamination in low microbial biomass microbiome studies: issues and recommendations. *Trends Microbiol.* **27**, 105–117 (2019).
 82. Labeda, D. P. & Goodfellow, M. in *Bergey's Manual of Systematics of Archaea and Bacteria* 1-7.

83. Rickard, A. H. et al. *Adhaeribacter aquaticus* gen. nov., sp. nov., a Gram-negative isolate from a potable water biofilm. *Int J. Syst. Evol. Microbiol* **55**, 821–829 (2005).
84. Guo, L. et al. Oligotrophic bacterium *Hymenobacter latericoloratus* CGMCC 16346 degrades the neonicotinoid imidacloprid in surface water. *AMB Express* **10**, 7 (2020).
85. Philippon, T. et al. Denitrifying bio-cathodes developed from constructed wetland sediments exhibit electroactive nitrate reducing biofilms dominated by the genera *Azoarcus* and *Pontibacter*. *Bioelectrochemistry* **140**, 107819 (2021).
86. Jurado, V., Miller, A. Z., Alias-Villegas, C., Laiz, L. & Saiz-Jimenez, C. *Rubrobacter bracarensis* sp. nov., a novel member of the genus *Rubrobacter* isolated from a biodeteriorated monument. *Syst. Appl Microbiol* **35**, 306–309 (2012).
87. de Vries, H. J. et al. Isolation and characterization of Sphingomonadaceae from fouled membranes. *npj Biofilms Microbiomes* **5**, 6 (2019).
88. Vacca, M. et al. The Controversial Role of Human Gut Lachnospiraceae. *Microorganisms* **8**, 573 (2020).
89. Baldani, J. I. et al. in *The Prokaryotes: Alphaproteobacteria and Betaproteobacteria* (eds Eugene Rosenberg et al.) 919–974 (Springer Berlin Heidelberg, 2014).
90. Dastager, S. G., et al. 455–498 (Springer Berlin Heidelberg, 2014).
91. Ivanova, N. et al. Complete genome sequence of *Geodermatophilus obscurus* type strain (G-20). *Stand Genom. Sci.* **2**, 158–167 (2010).
92. Alonso-Reyes, D. et al. Genomic Insights of an Andean Multi-resistant Soil Actinobacterium of Biotechnological Interest. bioRxiv, 2020.2012.2021.423370 (2020) <https://doi.org/10.1101/2020.12.21.423370>.
93. Kumar, C. G. & Sujitha, P. Kocuran, an exopolysaccharide isolated from *Kocuria rosea* strain BS-1 and evaluation of its in vitro immunosuppression activities. *Enzym. Micro. Technol.* **55**, 113–120 (2014).
94. Raguénès, G. et al. A novel exopolymer-producing bacterium, *Paracoccus zeaxanthinifaciens* subsp. *payriae*, isolated from a “kopara” mat located in Rangiroa, an atoll of French Polynesia. *Curr. Microbiol* **49**, 145–151 (2004).
95. Bailey, A. C. et al. Draft Genome Sequence of *Massilia* sp. Strain BSC265, Isolated from Biological Soil Crust of Moab, Utah. *Genome Announc* **2**, e01199–01114 (2014).
96. Deneff, V. J., Fujimoto, M., Berry, M. A. & Schmidt, M. L. Seasonal succession leads to habitat-dependent differentiation in ribosomal RNA:DNA Ratios among freshwater lake bacteria. *Front Microbiol* **7**, 606 (2016).
97. Salazar, G. et al. Particle-association lifestyle is a phylogenetically conserved trait in bathypelagic prokaryotes. *Mol. Ecol.* **24**, 5692–5706 (2015).
98. Schmidt, M. L., White, J. D. & Deneff, V. J. Phylogenetic conservation of freshwater lake habitat preference varies between abundant bacterioplankton phyla. *Environ. Microbiol.* **18**, 1212–1226 (2016).
99. Stepanauskas, R. et al. Improved genome recovery and integrated cell-size analyses of individual uncultured microbial cells and viral particles. *Nat. Commun.* **8**, 84 (2017).
100. Doughari, H. J., Ndakidemi, P. A., Human, I. S. & Benade, S. The ecology, biology and pathogenesis of *Acinetobacter* spp.: an overview. *Microbes Environ.* **26**, 101–112 (2011).
101. Bläckberg, A., Falk, L., Oldberg, K., Olaison, L. & Rasmussen, M. Infective endocarditis due to corynebacterium species: clinical features and antibiotic resistance. *Open Forum Infect. Dis.* **8** (2021) <https://doi.org/10.1093/ofid/ofab055>.
102. Zhang, Q. et al. *Hymenobacter xinjiangensis* sp. nov., a radiation-resistant bacterium isolated from the desert of Xinjiang, China. *Int J. Syst. Evol. Microbiol* **57**, 1752–1756 (2007).
103. Lee, J.-J. et al. *Hymenobacter aquaticus* sp. nov., a radiation-resistant bacterium isolated from a river. *Int. J. Syst. Evolut. Microbiol.* **67**, 1206–1211 (2017).
104. Alessa, O. et al. Comprehensive comparative genomics and phenotyping of methylbacterium species. *Front. Microbiol.* **12** (2021) <https://doi.org/10.3389/fmicb.2021.740610>.
105. Titécat, M., Wallet, F., Vieillard, M. H., Courcol, R. J. & Loiez, C. *Ruminococcus gnavus*: an unusual pathogen in septic arthritis. *Anaerobe* **30**, 159–160 (2014).
106. Weber, B. S., Harding, C. M. & Feldman, M. F. Pathogenic acinetobacter: from the cell surface to infinity and beyond. *J. Bacteriol.* **198**, 880–887 (2015).
107. Hacker, E., Antunes, C. A., Mattos-Guaraldi, A. L., Burkovski, A. & Tauch, A. *Corynebacterium ulcerans*, an emerging human pathogen. *Future Microbiol.* **11**, 1191–1208 (2016).
108. Smith, K. F. & Oram, D. M. in *Encyclopedia of Microbiology* (Third Edition) (ed Moselio Schaechter) 94–106 (Academic Press, 2009).
109. Kovaleva, J., Degener, J. E. & van der Mei, H. C. Methylbacterium and its role in health care-associated infection. *J. Clin. Microbiol* **52**, 1317–1321 (2014).
110. Dyer, J. & Harris, P. *Paracoccus yeei*—An emerging pathogen or incidental finding? *Pathology* **52**, S123 (2020).
111. Moradali, M. F., Ghods, S. & Rehm, B. H. A. *Pseudomonas aeruginosa* lifestyle: a paradigm for adaptation, survival, and persistence. *Front. Cellular Infect. Microbiol.* **7** (2017) <https://doi.org/10.3389/fcimb.2017.00039>.
112. Ryan, M. P. & Adley, C. C. *Sphingomonas paucimobilis*: a persistent Gram-negative nosocomial infectious organism. *J. Hosp. Infect.* **75**, 153–157 (2010).
113. Souto, A., Guinda, M., Mera, A. & Pardo, F. Septic arthritis caused by *Sphingomonas paucimobilis* in an immunocompetent patient. *Reumatol. Clin.* **8**, 378–379 (2012).
114. Lanoix, J. P. et al. *Sphingomonas paucimobilis* bacteremia related to intravenous human immunoglobulin injections. *Med Mal. Infect.* **42**, 37–39 (2012).
115. van Bruggen, A. H., Brown, P. R. & Jochimsen, K. N. Corky root of lettuce caused by strains of a gram-negative bacterium from muck soils of Florida, new york, and wisconsin. *Appl Environ. Microbiol* **55**, 2635–2640 (1989).
116. VAN BRUGGEN, A. H. C., JOCHIMSEN, K. N. & BROWN, P. R. *Rhizomonas suberifaciens* gen. nov., sp. nov., the Causal Agent of Corky Root of Lettuce. *Int. J. Syst. Evolut. Microbiol.* **40**, 175–188 (1990).
117. Davis, J. H. & Williamson, J. R. Structure and dynamics of bacterial ribosome biogenesis. *Philos. Trans. R Soc. Lond. B Biol. Sci.* **372** (2017) <https://doi.org/10.1098/rstb.2016.0181>.
118. Maitra, A. & Dill, K. A. Bacterial growth laws reflect the evolutionary importance of energy efficiency. *Proc. Natl Acad. Sci.* **112**, 406–411 (2015).
119. Klumpp, S. & Hwa, T. Traffic patrol in the transcription of ribosomal RNA. *RNA Biol.* **6**, 392–394 (2009).
120. Jia, Y. et al. Rare taxa exhibit disproportionate cell-level metabolic activity in enriched anaerobic digestion microbial communities. *mSystems* **4**, e00208–e00218 (2019).
121. Zhou, Y. et al. Profiling airborne microbiota in mechanically ventilated buildings across seasons in hong kong reveals higher metabolic activity in low-abundance bacteria. *Environ. Sci. Technol.* **55**, 249–259 (2021).
122. Fessler, M., Gummesson, B., Charbon, G., Svenningsen, S. L. & Sørensen, M. A. Short-term kinetics of rRNA degradation in *Escherichia coli* upon starvation for carbon, amino acid or phosphate. *Mol. Microbiol.* **113**, 951–963 (2020).
123. Lahtinen, S. J. et al. Degradation of 16S rRNA and attributes of viability of viable but nonculturable probiotic bacteria. *Let. Appl Microbiol* **46**, 693–698 (2008).
124. Li, R. et al. Comparison of DNA-, PMA-, and RNA-based 16S rRNA Illumina sequencing for detection of live bacteria in water. *Sci. Rep.* **7**, 5752 (2017).
125. McKillip, J. L., Jaykus, L. A. & Drake, M. rRNA stability in heat-killed and UV-irradiated enterotoxigenic *Staphylococcus aureus* and *Escherichia coli* O157:H7. *Appl Environ. Microbiol* **64**, 4264–4268 (1998).
126. Sheridan, G. E., Masters, C. I., Shallcross, J. A. & MacKey, B. M. Detection of mRNA by reverse transcription-PCR as an indicator of viability in *Escherichia coli* cells. *Appl. Environ. Microbiol.* **64**, 1313–1318 (1998).
127. Villarino, A., Bouvet, O. M., Regnault, B., Martin-Delautre, S. & Grimont, P. A. D. Exploring the frontier between life and death in *Escherichia coli*: evaluation of different viability markers in live and heat- or UV-killed cells. *Res Microbiol* **151**, 755–768 (2000).
128. Schostag, M. D., Albers, C. N., Jacobsen, C. S. & Priemé, A. Low turnover of soil bacterial rRNA at low temperatures. *Front. Microbiol.* **11** (2020) <https://doi.org/10.3389/fmicb.2020.00962>.
129. Emerson, J. B. et al. Schrödinger’s microbes: Tools for distinguishing the living from the dead in microbial ecosystems. *Microbiome* **5**, 86 (2017).
130. Wang, Y. et al. Characterizing microbial community viability with RNA-based high-throughput sequencing. *Microbiome* Version 1, posted 22 Jul, 2022 (2022) <https://doi.org/10.21203/rs.3.rs-1870950/v1>.
131. Mbareche, H., Veillette, M., Bilodeau, G. J., Duchaine, C. & Schaffner, D. W. Bioaerosol sampler choice should consider efficiency and ability of samplers to cover microbial diversity. *Appl. Environ. Microbiol.* **84**, e01589–01518 (2018).
132. Pan, M., Lednický, J. A. & Wu, C.-Y. Collection, particle sizing and detection of airborne viruses. *J. Appl. Microbiol.* **127**, 1596–1611 (2019).
133. Nieto-Caballero, M., Savage, N., Keady, P. & Hernandez, M. High fidelity recovery of airborne microbial genetic materials by direct condensation capture into genomic preservatives. *J. Microbiol Methods* **157**, 1–3 (2019).
134. Šantl-Temkiv, T., Gosewinkle, U., Starnawski, P., Lever, M. & Finster, K. Aeolian dispersal of bacteria in southwest Greenland: their sources, abundance, diversity and physiological states. *FEMS Microbiol Ecol* **94** (2018) <https://doi.org/10.1093/femsec/fiy031>.
135. Maki, T. et al. Aeolian dispersal of bacteria associated with desert dust and anthropogenic particles over continental and oceanic surfaces. *J. Geophys. Res.: Atmospheres* **124**, 5579–5588 (2019).
136. Gonzalez-Martin, C., Teigell-Perez, N., Valladares, B. & Griffin, D. W. in *Advances in Agronomy* Vol. 127 (ed Donald Sparks) 1–41 (Academic Press, 2014).
137. Tisch Environmental, I. (2004).

138. Krasnov, H., Katra, I. & Friger, M. Increase in dust storm related PM10 concentrations: A time series analysis of 2001–2015. *Environ. Pollut.* **213**, 36–42 (2016).
139. Varga, G., Újvári, G. & Kovács, J. Spatiotemporal patterns of Saharan dust outbreaks in the Mediterranean Basin. *Aeolian Res.* **15**, 151–160 (2014).
140. Dayan, U. & Levy, I. Relationship between synoptic-scale atmospheric circulation and ozone concentrations over Israel. *J. Geophys. Res.: Atmospheres* **107**, ACL 31–31–ACL 31–12 (2002).
141. Klein, A. M., Bohannon, B. J. M., Jaffe, D. A., Levin, D. A. & Green, J. L. Molecular Evidence for Metabolically Active Bacteria in the Atmosphere. *Front. Microbiol.* **7** (2016) <https://doi.org/10.3389/fmicb.2016.00772>.
142. Luhung, I. et al. Experimental parameters defining ultra-low biomass bioaerosol analysis. *npj Biofilms Microbiomes* **7**, 37 (2021).
143. Stein, A. F. et al. Noaa's Hysplit Atmospheric Transport and Dispersion Modeling System. *Bull. Am. Meteorological Soc.* **96**, 2059–2077 (2015).
144. Rolph, G., Stein, A. & Stunder, B. Real-time Environmental Applications and Display sYstem: READY. *Environ. Model. Softw.* **95**, 210–228 (2017).
145. Acker, J. G. & Leptoukh, G. Online analysis enhances use of NASA Earth science data. *Eos, Trans. Am. Geophys. Union* **88**, 14–17 (2007).
146. Brauer, S. L. et al. Culturable *Rhodobacter* and *Shewanella* species are abundant in estuarine turbidity maxima of the Columbia River. *Environ. Microbiol.* **13**, 589–603 (2011).
147. Caporaso, J. G. et al. Ultra-high-throughput microbial community analysis on the Illumina HiSeq and MiSeq platforms. *ISME J.* **6**, 1621–1624 (2012).
148. Soergel, D. A. W., Dey, N., Knight, R. & Brenner, S. E. Selection of primers for optimal taxonomic classification of environmental 16S rRNA gene sequences. *ISME J.* **6**, 1440–1444 (2012).
149. Callahan, B. J. et al. DADA2: High-resolution sample inference from Illumina amplicon data. *Nat. Methods* **13**, 581 (2016).
150. McMurdie, P. J. & Holmes, S. phyloseq: an R package for reproducible interactive analysis and graphics of microbiome census data. *PLoS One* **8**, e61217 (2013).
151. Quast, C. et al. The SILVA ribosomal RNA gene database project: improved data processing and web-based tools. *Nucleic Acids Res.* **41**, D590–D596 (2013).
152. Davis, N. M., Proctor, D. M., Holmes, S. P., Relman, D. A. & Callahan, B. J. Simple statistical identification and removal of contaminant sequences in marker-gene and metagenomics data. *Microbiome* **6**, 226 (2018).
153. Martin-Fernandez, J. A., Hron, K., Templ, M., Filzmoser, P. & Palarea-Albaladejo, J. Bayesian-multiplicative treatment of count zeros in compositional data sets. *Stat. Model.* **15** (2015) <https://doi.org/10.1177/1471082x14535524>.
154. Palarea-Albaladejo, J. & Martin-Fernandez, J. A. zCompositions—R Package for multivariate imputation of left-censored data under a compositional approach. *Chemometrics Intell. Lab. Syst.* **143**, 85–96 (2015).
155. van den Boogaart, K. G. & Tolosana-Delgado, R. “compositions”: A unified R package to analyze compositional data. *Comput. Geosci.* **34**, 320–338 (2008).
156. Amato, P. et al. In *Microbiology of Aerosols* 1–21 (2017).
157. Rao, A. K. & Whitby, K. T. Nonideal collection characteristics of single stage and cascade impactors. *Am. Ind. Hyg. Assoc. J.* **38**, 174–179 (1977).
158. Jari Oksanen, F. G. B. et al. *vegan*: Community Ecology Package. (2020).
159. Gilmour, S. G. In *Wiley StatsRef: Statistics Reference Online*.
160. Margolin, B. H. In *Wiley StatsRef: Statistics Reference Online*.
161. Benjamini, Y. & Hochberg, Y. Controlling the false discovery rate: a practical and powerful approach to multiple testing. *J. R. Stat. Soc. Ser. B (Methodol.)* **57**, 289–300 (1995).

162. Mallick, H. et al. Multivariable association discovery in population-scale meta-omics studies. *PLoS Comput. Biol.* **17**, e1009442 (2021).

Acknowledgements

This study was partially supported by the Israel Science Foundation (grant 928/21), the Helmholtz Zentrum München and the Helmholtz Association (Berlin, Germany) in the framework of the AeroHEALTH Helmholtz International Lab (InterLabs-0005), a German-Israeli project. YR acknowledges support from the de Botton Center for Marine Sciences (Weizmann Institute) and a research grant from the Estate of Raymond Lapon and the Estate of Betty Weneser.

Author contributions

Conceptualization: B.A.E., D.G. and Y.R.; Methodology: B.A.E., D.G. and Y.R.; Investigation: B.A.E. and D.G.; Data curation: B.A.E. and D.G.; Writing-original draft: B.A.E.; Visualization: B.A.E.; Writing-review and editing: B.A.E., D.G. and Y.R.; Resources: Y.R.

Competing interests

The authors declare no competing of interest. Y.R. is an Editorial Board Member for *Communications Earth & Environment*, but was not involved in the editorial review of, nor the decision to publish this article.

Additional information

Supplementary information The online version contains supplementary material available at <https://doi.org/10.1038/s43247-023-00679-8>.

Correspondence and requests for materials should be addressed to Yinon Rudich.

Peer review information *Communications Earth & Environment* thanks Katsuro Hagiwara, David Cappelletti and the other, anonymous, reviewer(s) for their contribution to the peer review of this work. Primary Handling Editors: Clare Davis.

Reprints and permission information is available at <http://www.nature.com/reprints>

Publisher's note Springer Nature remains neutral with regard to jurisdictional claims in published maps and institutional affiliations.



Open Access This article is licensed under a Creative Commons Attribution 4.0 International License, which permits use, sharing, adaptation, distribution and reproduction in any medium or format, as long as you give appropriate credit to the original author(s) and the source, provide a link to the Creative Commons license, and indicate if changes were made. The images or other third party material in this article are included in the article's Creative Commons license, unless indicated otherwise in a credit line to the material. If material is not included in the article's Creative Commons license and your intended use is not permitted by statutory regulation or exceeds the permitted use, you will need to obtain permission directly from the copyright holder. To view a copy of this license, visit <http://creativecommons.org/licenses/by/4.0/>.

© The Author(s) 2023